

# Multiscale Attention via Wavelet Neural Operators for Vision Transformers

Anahita Nekoozadeh<sup>1</sup>, Mohammad Reza Ahmadzadeh<sup>1</sup>, Zahra Mardani<sup>2</sup>, Morteza Mardani<sup>3</sup>

<sup>1</sup>Department of Electrical and Computer Engineering, Isfahan University of Technology, Isfahan, Iran,

<sup>2</sup>ISCTE-University Institute of Lisbon(Instituto Universitário de Lisboa), <sup>3</sup>Stanford University

a.nekozadeh@ec.iut.ac.ir, Ahmadzadeh@iut.ac.ir, zmardani@lnec.pt, morteza@stanford.edu

## Abstract

*Transformers have achieved widespread success in computer vision. At their heart, there is a Self-Attention (SA) mechanism, an inductive bias that associates each token in the input with every other token through a weighted basis. The standard SA mechanism has quadratic complexity with the sequence length, which impedes its utility to long sequences appearing in high resolution vision. Recently, inspired by operator learning for PDEs, Adaptive Fourier Neural Operators (AFNO) were introduced for high resolution attention based on global convolution that is efficiently implemented via FFT. However, the AFNO global filtering cannot well represent small and moderate scale structures that commonly appear in natural images. To leverage the coarse-to-fine scale structures we introduce a Multiscale Wavelet Attention (MWA) by leveraging wavelet neural operators which incurs linear complexity in the sequence size. We replace the attention in ViT with MWA and our experiments with CIFAR and ImageNet classification demonstrate significant improvement over alternative Fourier-based attentions such as AFNO and Global Filter Network (GFN).*

## 1. Introduction

The success of transformer networks in Natural Language Processing (NLP) tasks has motivated their application to computer vision. Among the prominent advantages of transformers is the possibility of modeling long-range dependencies among the input sequence and supporting parallel processing compared to Recurrent Neural Networks (RNN). In addition, unlike Convolutional Neural Networks (CNN), they require minimal inductive biases for their design. The simple design of transformers also enables processing of multi-modality contents (such as images, video, text, and speech) by using the same processing blocks. It exhibits excellent scalability for large-size netwo-

rks trained with huge datasets. These strengths have led to many improvements in vision benchmarks using transformer networks [25, 9, 6].

A key component for the effectiveness of transformers is the proper mixing of tokens. Finding a good mixer is challenging because it needs to scale with the sequence size. The Self-Attention (SA) block in the original transformer suffers from quadratic complexity. In order to make mixing efficient, several ideas have been introduced. Recently, Adaptive Fourier Neural Operator (AFNO) have been proposed to replace SA by leveraging the geometric structure of images via learning a global convolution operator in the Fourier space. As a major shortcoming of AFNO, it is a global operator, and thus can miss the fine and moderate scale structures that are quite present in natural images [5, 9].

To overcome the shortcomings of AFNO, one needs to effectively mix tokens at different scales [5]. To this end, we propose the use of wavelet transform, which is known as an effective multiscale representation for natural images in image processing. In order to learn a multiscale mixer, we adapt a variation of Wavelet Neural Operator (WNO) that has been studied for solving PDEs in fluid mechanics [24]. We modify the design to account for high-resolution natural images with discontinuities due to objects and edge structures. After the architectural modifications, the MWA attention layer is shown in Fig. 1.

The input image is first transformed into the wavelet domain using two-dimensional Discrete Wavelet Transform (2D-DWT). Then, all coefficients from the last decomposition level are convolved with the learnable weights, and subsequently undergo a nonlinear GeLU activation. Then, an inverse 2D-DWT reconstructs the pixel level tokens. For 2D-DWT (and its inverse), we choose Haar wavelet with decomposition level  $m=1$  for faster speed. We conducted experiments for classification, and the experiments show that our MWA has a better performance and accuracy than SA block [3] and Fourier based attentions including AFNO [5] and the Global Filter Network (GFN) [18].

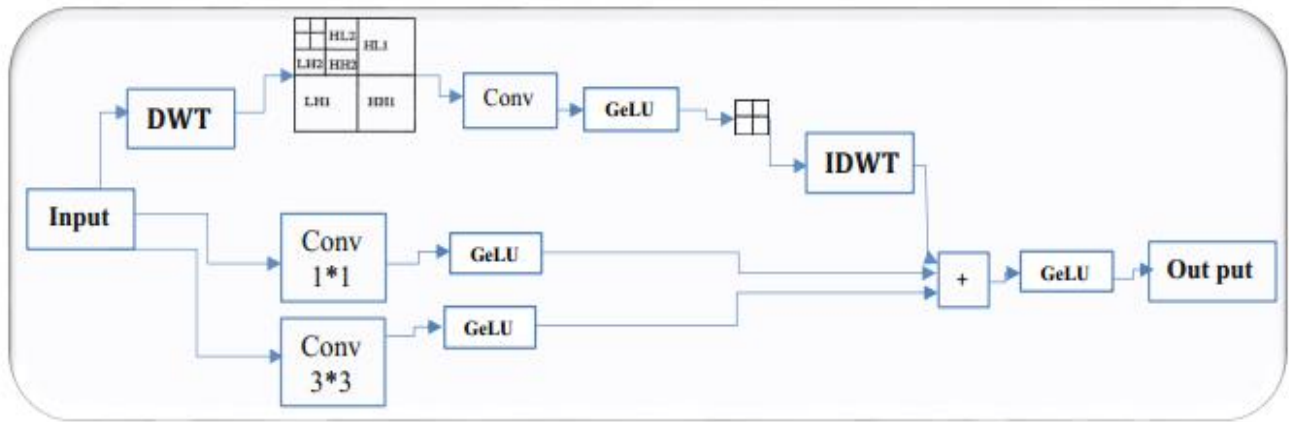
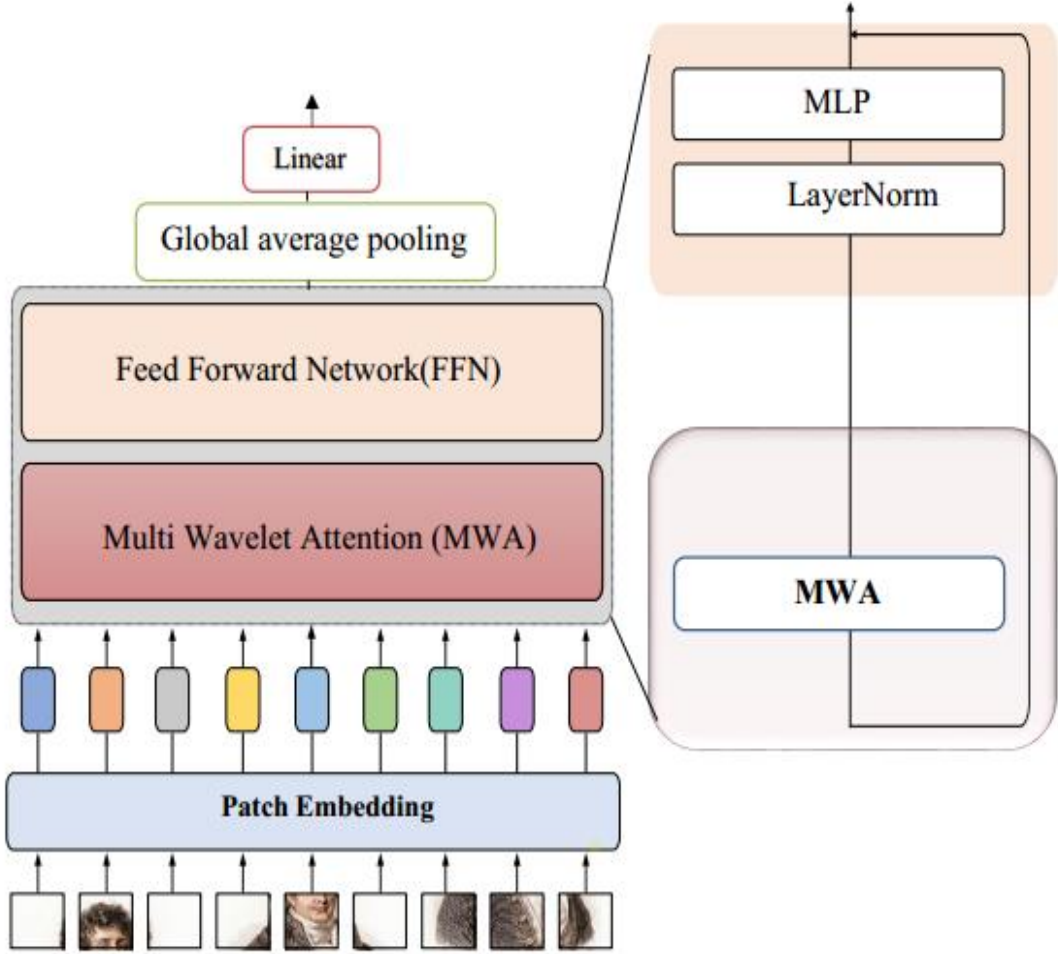


Figure 1. The general architecture of our Multiscale Wavelet Attention (MWA) for vision transformers. The bottom diagram shows the MWA architecture. Tokens are first spatially mixed using 2D-DWT. Then the tokens are filtered in the wavelet space by convolving all the coefficients of the last level of decomposition with learnable weights followed by a nonlinear GeLU activation. Then, 2D-DWT is applied to reconstruct the spatial pixel-level tokens. Weighted skip connections are also added to facilitate learning the identity map and high frequency details in the output.

The comparison of MWA with AFNO, GFN and SA block is mentioned in Tab. 1 in terms of the number of parameters and complexity.

## 2. Related Works

Several works have been introduced to improve the efficiency of the attention mechanism in transformers. We divide them into three main categories.

**Graph based attention.** graph-based SA methods include: (1) sparse attention with fixed patterns; which reduces the attention by limiting the field-of-view to predetermined patterns such as local windows in sparse transformers [2]; (2) sparse attention with learnable patterns; where a fixed pattern is learned from data; e.g., axial transformer [7] and reformers [10]; (3) memory; another prominent method is to use a peripheral memory module that can access multiple tokens at the same time. A common form is global memory that can access the entire sequence e.g., set transformers [12]; (4) low-rank methods approximate the SA via a low-rank matrix; e.g., linformers [26]; (5) kernel methods; use kernel trick to approximate linear transformers [8]; (6) recurrence is another method to improve the efficiency of the transformer e.g., compressive transformer [17].

**MLP based attention.** Several works have recently been proposed that use MLP to replace self-interacting layers in feature transformation and fusion, such as ResMLP [23], which replaces layer normalization with affine transformation. A recently proposed gMLP [15] also uses a spatial gating unit to reweight features in the spatial dimension. However, all models including MLP that are used to combine tokens spatially have two basic drawbacks: (1) Similar to SA, MLPs still require quadratic complexity with the sequence size; (2) MLP mixers have static weights, and they are not dynamic with respect to the input.

**Fourier based attention.** Recently, FNet, GFN, and AFNO models have been presented, which incur linear complexity. FNet [13] is an efficient transformer where each layer consists of a Fourier transform sublayer followed by a feedforward sublayer. Basically, the SA layers are replaced by Fourier transform with no learnable weights, and two-dimensional Discrete Fourier Transform (2D-DFT) is applied to embed the sequence length and hidden dimension.

Another efficient transformer is the Global Filter Network (GFN), which aims to replace SA with a static global convolution filter. GFN however lacks adaptivity [18].

AFNO, was introduced from the operator learning perspective to solve the shortcomings of GFN, by introducing weight sharing and block diagonal structure on the learnable weights that makes it scalable [5]. AFNO however, suffers from global biases and does not represent multiscale appearing commonly in natural images. The novelty of our

proposed method is to account for multiscale structures using MWA attention.

## 3. Preliminaries and problem statement

Consider a two-dimensional  $3 \times m \times n$  RGB image  $x$  that is divided into small and non-overlapping patches. After patching with patch size  $p$ , the image can be seen as a two-dimensional grid  $3 \times h \times w$ , where  $h = m/p$ , and  $w = n/p$ . Each RGB patch then undergoes a linear projection that creates tokens with a  $d$ -dimensional embedding, namely  $d \times h \times w$ . In order to preserve the position information, a  $d$ -dimensional position embedding is also added to each token. Since then, the transformer network processes the two-dimensional sequence of tokens by mixing them over the layers using the attention module that creates the final representation for end tasks [5, 9, 21].

SA learns similarity among tokens [6]. However, quadratic complexity with the sequence size hinders the training of high-resolution images [22]. Our goal is to replace attention with a compute and memory efficient module that is aware of the multiscale structures in the natural images for downstream tasks. Before delving into the details of multiscale attention, let us overview global-scale attention based on AFNO.

### 3.1. Adaptive Fourier Neural Operator

Neural operators learn the mapping between two functions in continuous space [1]. They are trained only once and once after training, they can do prediction for any input function. Neural operators are typically used for solving PDEs. They can also be extended to computer vision, since images can be treated as RGB-valued functions [14]. This generalization allows us to take advantage of operator learning in computer vision.

In order to leverage the geometric structure of images, the AFNO, relies on convolution with a global filter that is as big as the input tokenized image. AFNO efficiently implements global convolution via FFT, which is inspired by the Fourier Neural Operator (FNO). However, FNO has a  $d \times d$  weight matrix for each token ( $d = n/p$  is the token grid dimension), so the number of parameters becomes very large for high resolution inputs. To reduce the number of parameters, AFNO imposes a block-diagonal structure on the weights. It then shares the weights among the features and truncates certain frequency components using soft-thresholding and shrinkage operations [5]. However, FFT is not suitable to represent images with non-periodic patterns. Natural images usually exhibit multiscale structures, and AFNO can miss non-periodic and small-to-medium scale structures. To model multiscale structures, our idea is to leverage wavelet transform and consequently the wavelet neural operators, that take advantage of wavelets and have

been very successful for solving PDEs with sudden changes as discussed in the next part.

## 4. Wavelet transform and Wavelet Neural Operator

### 4.1. Wavelet transform for signal representation

Let  $\psi(x) \in L^2(\mathbb{R})$  be a canonical mother wavelet that is local in both time and frequency domains. Let also  $W(\Gamma)$  and  $W^{-1}(\Gamma_w)$  be the forward wavelet transform and the inverse wavelet transform of an arbitrary function  $\Gamma: D \rightarrow \mathbb{R}^d$ . Then, the wavelet transform and the inverse are the transforms of the function  $\Gamma$  with scaling and displacement parameters  $\alpha \in \mathbb{R}$  and  $\beta \in \mathbb{R}$ . They are obtained as follows using the following integral pairs [24],

$$(W^{-1}\Gamma)(x) = \frac{1}{C_\psi} \iint_0^{+\infty} \Gamma_w(\alpha, \beta) \frac{1}{\sqrt{|\alpha|}} \tilde{\psi}\left(\frac{x-\beta}{\alpha}\right) d\beta \frac{d\alpha}{\alpha^2} \quad (1)$$

$$(W\Gamma)(\alpha, \beta) = \int_D \Gamma(x) \frac{1}{\sqrt{|\alpha|}} \psi\left(\frac{x-\beta}{\alpha}\right) dx \quad (2)$$

Where  $(\Gamma_w)(\alpha, \beta) = (W\Gamma)(\alpha, \beta) \psi((x - \beta)\alpha) \in L^2(\mathbb{R})$  is scaled and transferred to the mother wavelet. By scaling and shifting, the desired wavelets can be obtained from the mother wavelet. Each set of wavelet functions forms an orthogonal set of basis functions.

Note; that term  $C_\psi$  is the admissible constant which ranges in  $0 \leq C_\psi \leq \infty$ . The expression for  $C_\psi$  is given as follows,

$$C_\psi = 2\pi \int_D \frac{|\psi(\omega)|^2}{|\omega|} d\omega \quad (3)$$

In signal representation theory, wavelet decomposition has proven successful in compressible representation with a few basis functions compared with Fourier transform. This comes from the nature of wavelet bases that can well represent trends, breakpoints, and discontinuities in higher derivatives and similarities [28]. We aim to rely on the spatial and frequency localization power of wavelets to learn the relationship between tokens and thus learn the multiscale patterns at the internal layers of transformers. Considering these features, we adapt the WNO, which we discuss in the next section [24, 4, 20].

### 4.2. Wavelet Neural Operator

The class of shift-equivariant kernels has the favorable property that they can be analyzed as linear combinations of eigen functions [19]. A powerful class of eigen function are the wavelet transform bases, where according to the co-

nvolution theorem, multiscale convolution in the spatial domain is equal to multiplication in the wavelet transform domain. Accordingly, the WNO can be defined next [24].

**Definition (Kernel integral operator).** The kernel integral operator  $K$  is defined as follows:

$$K(x)(s) = \int_D k(s; t)x(t)dt; \quad s \in D \quad (4)$$

With a continuous kernel function  $k: D \times D \rightarrow \mathbb{R}^{d \times d}$ . For the special case of Green's kernel,  $k(s; t)$  can be expressed as  $k(s; t) = k(s - t)$ , and the integral of Equ. (4) leads to multiscale convolution defined below.

**Definition (Multiscale convolution kernel operator).** Assuming that as  $k(s; t) = k(s - t)$ , The kernel integral of Equ. (4) is rewritten as follows:

$$K(x)(s) = \int_D k(s - t)x(t)dt; \quad s \in D \quad (5)$$

The Green's kernel has a useful regularization effect that can capture multi-scale interactions. In addition, it can be used to effectively implement multiscale convolution using Discrete Wavelet Transform (DWT).

**Definition (Wavelet neural operator).** For the continuous input  $x \in D$  and kernel  $k$  and the kernel integral at token  $s$ , the wavelet neural operator is defined as follows:

$$K(x)(s) = W^{-1}(W(x) \cdot W(k))(s); \quad s \in D \quad (6)$$

Here,  $\cdot$  denotes matrix multiplication, and  $W$  and  $W^{-1}$  represent the forward DWT and the inverse DWT.

## 5. Multiscale Wavelet Attention

Inspired by WNO, for RGB images, our idea is to combine the tokens using DWT. We make fundamental modifications to adapt the WNO operator to images to account for high-resolution natural images with object-induced discontinuities and edge structures. In the proposed MWA, for faster and better performance, we use 2D-DWT to combine tokens. 2D-DWT enjoys fast implementations with GPU support [11].

In MWA, images are converted into high-frequency and low-frequency components using 2D-DWT. In essence, high-frequency components represent edges in the image, while low-frequency components represent smooth regions. According to Fig. 1, the first branch in the two-dimensional array calculates four components as follows: the approximation component (LL) that represent low frequency components; the detail components that account for high frequencies such as horizontal (HL), vertical (LH) and diagonal (HH). In this work, we use all the coefficients of the last decomposition level. In DWT, we transform the mother wavelet to calculate the wavelet coefficients on scales with powers of two. In this case, the wavelet  $\varphi(x)$  is

Table 1. Complexity, parameter count, and interpretation for MWA, AFNO, GFN, and SA.  $N = hw$ ,  $d$  and  $K$  refer to the sequence size, channel size, and block count in AFNO. Also,  $k_1$ ,  $k_2$  are kernel size for MWA, and  $g_1, g_2$  is the number of groups, respectively.

| Models | Complexity (FLOPs)                                | Parameter Count              | Interpretation        |
|--------|---|------------------------------|-----------------------|
| SA     | $N^2d + 3Nd^2$                                    | $3d^2$                       | Graph Global Conv     |
| GFN    | $Nd + Nd \log N$                                  | $Nd$                         | Depthwise Global Conv |
| AFNO   | $Nd^2 / k + Nd \log N$                            | $(1 + 4 / k)d^2 + 4d$        | Adaptive Global Conv  |
| MWA    | $1 \cdot 5k_1Nd^2 / g_1 + 1 \cdot 5k_2Nd^2 / g_2$ | $(k_1 / g_1 + k_2 / g_2)d^2$ | Multi Scale Conv      |

defined as follows [24]:

$$\psi_{m,t}(x) = \frac{1}{\sqrt{2^m}} \psi\left(\frac{x-t2^m}{2^m}\right) \quad (7)$$

Where the parameters  $m$  and  $t$  are the scaling and shifting parameters and the forward DWT wavelet transform is shown below [24]:

$$(W\Gamma)(m,t) = \frac{1}{\sqrt{2^m}} \int_D \Gamma(x) \psi\left(\frac{x-t2^m}{2^m}\right) dx \quad (8)$$

By fixing the scale parameter  $m$  in a certain integer and shifting  $t$ , the DWT coefficients at the level of  $m$  can be obtained. Since the use of a one-way filter bank is very effective for decomposing a signal into multiple frequency subbands, 2D-DWT is implemented as a filter bank, which works as a sequence of low-pass and high-pass filters. In the implementation of the filter bank, by passing the image through a low-pass filter and a high-pass filter, the image is decomposed into details and approximate coefficients. If  $r(n)$  and  $s(n)$  represent low-pass and high-pass filters, respectively, then two convolutions in the form  $z_{high}(n) = (x * s)(n)$  and  $z_{low}(n) = (x * r)(n)$  are executed, where  $n$  is the number of discretization points. While the detail coefficients  $z_{high}(n)$  are preserved, the approximate coefficients  $z_{low}(n)$  are recursively filtered by passing it through low-pass and high-pass filters until the total number of decomposition levels is exhausted [24, 16, 29]. At each level, the length of the image is halved due to conjugate symmetry. The general architecture of the MWA model is shown in Fig. 1.

Our model takes non-overlapping  $h \times w$  grid of patches as input and project each patch into  $d$  dimensional space. We define the input token tensor  $x \in R^{h \times d \times w}$  and the weight tensor  $w \in R^{(h \times w / 2^m) \times d \times d}$  for parameterization of the kernel. MWA performs a sequence of operations for Each token  $(m,n) \in [w] \times [h]$ , which we will discuss below.

**First step:** Unlike AFNO, which combines tokens with Discrete Fourier Transform (DFT), MWA combines tokens representing different spatial locations using DWT as

$$z_{m,n} = [DWT(x)]_{m,n} \quad (9)$$

Only from the wavelet coefficients with the highest scale, a parametrization space with limited dimension is obtained.

In general, the length of the wavelet coefficients are also affected by the number of vanishing moments of the orthogonal mother wavelet. Thus, we use the coefficients  $z_{m,n}$  at the highest level of analysis.

**Second step:** While AFNO uses the multiplication between the learnable weight tensor and the coefficients obtained from the DFT, we use the convolution between a learnable weight tensor and coefficients of the last level of decomposition as follows:

$$\tilde{z}_{m,n} = z_{m,n} * w_{m,n} \quad (10)$$

**Third step:** Unlike AFNO, which uses Inverse Discrete Fourier Transform (IDFT) to recover tokens after mixing, we use Inverse Discrete Wavelet Transform (IDWT) to update and separate tokens by using:

$$y_{m,n} = [IDWT(\tilde{z})]_{m,n} \quad (11)$$

Using 2D-DWT, we can generate fine image details as well as the rough approximation of the image. Note, DWT and IDWT are well supported by CPU and GPU, so the proposed model has good performance on hardware.

**Fourth step:** weighted skip connections are added using two convolution layers with different kernel sizes (second and third branches of Fig. 1). These convolution layers facilitate learning the identity mapping and have been proven useful for learning high frequency details.

In general, the architectural highlights are as follows:

- Network parameters are learned in the wavelet space, which are localized both in frequency and spatial domains, and thus they can learn multiscale patterns in images effectively.
- WNO is adopted from continuous PDEs and modified for discrete images by adding more nonlinearity and adding convolutional skip connections. Also, both the approximation and detail coefficients of the wavelet transform are used to model the attention.
- Our model is more flexible than SA because both DWT and IDWT have no learnable parameters and can process sequences with arbitrary length.

## 6. Complexity

In this section we quantify the operation count for the proposed MWA attention. For DWT, the input is simultaneously decomposed using a low-pass filter  $r(n)$  and a high-pass filter  $s(n)$ . In case of Haar Wavelet, the high-pass and low-pass filters have a fixed length, each of which perform  $z_{high}(n) = (r * x)(n)$  and  $z_{low}(n) = (s * x)(n)$ , which  $O(N)$  complexity for the sequence size  $N$ . DWT also uses these two filters for decomposition. Thus, the implementation of DWT filter bank has complexity of  $O(N)$  [28]. Decomposing the input using a wavelet with level  $m$  results in an image of length  $n/2^m$ .

The convolution of the analyzed coefficients of the last level and the weights has a complexity of  $O(KNd^2 / 2mg)$  (in our proposed architecture, the level of analysis is  $m=1$ ). The decomposition level and number of groups plays an important role in increasing the speed of our proposed architecture. The input convolution and weights with the kernel size  $k$  and the number of groups  $g$  also have complexity  $O(kNd^2 / g)$  [27]. The overall complexity of the architecture is shown in Tab. 1.

## 7. Experiments

We conduct experiments to confirm the effectiveness of MWA and compare the results with different Fourier based transformers. We perform our experiment on CIFAR and Tiny-ImageNet datasets as widely used small and medium-scale benchmarks for image classification.

**Datasets.** As mentioned, we adopt CIFAR and Tiny-ImageNet datasets. CIFAR-10 contains 60,000 images from 10 class categories, while CIFAR-100 contains 60,000 from 100 class categories. Tiny-ImageNet also contains 100,000 images with 200 classes. We report the accuracy on test data.

**Comparisons.** We compare our method with the attention block in the main transformer and the AFNO and GFN Fourier transform methods, which have similar FLOPs and

number of parameters, and we see that our method can clearly perform well in small and medium sized data such as CIFAR and Tiny-ImageNet (see Tab. 2, Tab. 3 and Tab. 4). One of the problems with transformers is that they require a lot of data for training, and they perform poorly on medium and low data, but our method can perform better than previous transformers on small datasets.

### 7.1. Architecture and training

The proposed MWA block consists of three major components. The first component converts the input image taken from the previous layer into a wavelet domain using 2D-DWT (horizontal, vertical and diagonal approximation coefficients and details). Then convolution is performed on all the approximate coefficients and details of the last level of decomposition and learnable weights, which then undergo GeLU nonlinear activation. Then, an inverse 2D-DWT reconstructs the pixel-level tokens. For 2D-DWT and its inverse, we choose Haar Wavelet with decomposition level  $m = 1$ . For skip connections we use two-dimensional convolution with a different kernel sizes  $1 \times 1$  and  $3 \times 3$ , followed by nonlinear GeLU activation. Finally, all three branches are gathered and passed through a non-linear GeLU activation.

We use the ViT-S/4 configuration for experimenting on CIFAR10-100 and Tiny-ImageNet datasets. The ViT-S/4 configuration has 12 layers and a hidden size of 384, and a token size of  $4 \times 4$  is used to model the sequence size. We use global average pooling at the last layer to produce output softmax probabilities for classification.

We trained all models for 300 epochs with Adam optimizer and cross-entropy loss using a learning rate of  $5 \times 10^{-4}$ . We also use five epochs of linear learning-rate warm-up. We use a cosine decay schedule with a minimum value of  $10^{-5}$ , along with a smooth gradient cut-off to stabilize the training that does not exceed a value of 1, and the weight-decay regularization is set to 0.05.

In particular, we use 12 transformer layers and adjust the hyperparameters of interest in AFNO and MWA to achieve a close and comparable number of parameters. More details about each model are provided below.

- SA uses 8 attention heads and a hidden size of 384 [3].
- GFN uses a hidden size of 384 [18].
- AFNO uses a hidden size 384, and a sparsity threshold of 0.1 (with 3-4 blocks to reach 16M-17M parameters) [5].
- MWA uses a hidden size 384, 2D ensemble convolution with kernel size 3 and 1 as learnable weights (together with a different number of groups to arrive at a parameter count of 16-17M).

Table 2. Comparisons of different transformer-style architectures for image classification on CIFAR-100. All our models are trained on  $32 \times 32$  images at 300 epochs and patch size 4. All experiments are performed on 1 GPU.

| Model       | Parameters (M) | Flops (G) | Top-1 (%)   | Top-5 (%) |
|-------------|----------------|-----------|-------------|-----------|
| <b>SA</b>   | 21             | 1.40      | 60.6        | 82.32     |
| <b>GFN</b>  | 15             | 0.9       | 71.2        | 88.03     |
| <b>AFNO</b> | 16             | 1.052     | 71.9        | 89.20     |
| <b>MWA</b>  | 16             | 1.094     | <b>73.2</b> | 88.45     |

Table 3. Comparisons of different transformer-style architectures for image classification on CIFAR-10. All our models are trained on  $32 \times 32$  images at 300 epochs and patch size 4. All experiments are performed on 1 GPU.

| Model       | Parameters (M) | Flops (G) | Top-1 (%)   | Top-5 (%) |
|-------------|----------------|-----------|-------------|-----------|
| <b>SA</b>   | 21             | 1.40      | 88.0        | 99.30     |
| <b>GFN</b>  | 15             | 0.9       | 94.4        | 99.69     |
| <b>AFNO</b> | 16             | 1.052     | 93.7        | 99.67     |
| <b>MWA</b>  | 16             | 1.094     | <b>95.7</b> | 99.70     |

Note that the ViT backbone used in our experiments has a patch size of 4 compared to the patch size of 16 used in the original ViT architecture for image classification. As a result, we observe that self-attention performs poorly compared with MWA and Fourier based methods.

## 7.2. CIFAR Classification

Table 4. Comparisons of different transformer-style architectures for image classification on Tiny-ImageNet. All our models are trained on  $64 \times 64$  images at 300 epochs and patch size 4. All experiments are performed on 1 GPU.

| Model       | Parameters (M) | Flops (G) | Top-1 (%)   | Top-5 (%) |
|-------------|----------------|-----------|-------------|-----------|
| <b>SA</b>   | 21             | 6.057     | 45.7        | 68.06     |
| <b>GFN</b>  | 16             | 3.64      | 59.7        | 78.15     |
| <b>AFNO</b> | 17             | 4.32      | 59.4        | 79.8      |
| <b>MWA</b>  | 17             | 4.54      | <b>60.7</b> | 79.03     |

We perform image classification experiments with the MWA mixer module and using the backbone ViT-S/4 on the CIFAR-10 and CIFAR-100 dataset containing 10,000 test sets with 10 and 100 classes, respectively, with resolution  $32 \times 32$ . We measure performance using top-1 and top-5 accuracy along with flops for different model parameters.

**CIFAR classification:** Classification results for different mixers are shown Tab. 2 and Tab. 3. It can be seen that the proposed MWA using DWT, can learn multiscale as well as non-periodic patterns in the images better than the Fourier transform, which leads to higher than 1% accuracy improvements over existing Fourier-based mixers such as AFNO and GFN.

## 7.3. Tiny-ImageNet classification

We perform image classification experiments with the MWA mixer module and using the backbone ViT-S/4 on the Tiny-ImageNet dataset that contains 100,000 images of 200 classes downsized to  $64 \times 64$  colored images. Each class has 500 training images, 50 validation images and 50 test images. We measure performance through top-1 and top-5 validation accuracy along with flop and model parameters.

**Tiny-ImageNet classification:** Classification results for different mixers are shown in Tab. 4. It is observed that our proposed MWA, thanks to multiscale wavelet features that exist in natural images, outperforms global Fourier based methods including AFNO and GFN by more than 1% in top-1 accuracy. It also significantly outperforms SA when the patch size is chosen to be 4.

## 8. Conclusions

We introduced Multiscale Wavelet Attention (MWA) for transformers to effectively learn small-to-large range dependencies among the image pixels for representation learning. MWA adapts wavelet neural operators from PDEs and fluid mechanics after making basic corrections to WNO for natural images. MWA incurs linear complexity in the sequence size and enjoys fast algorithms for wavelet transform.

Our experiments for image classification on CIFAR and ImageNet data show the superior accuracy of our proposed MWA block compared with alternative Fourier based attentions. There are still important directions to pursue. One of those pertains to more extensive evaluations with larger datasets and complex images involving multiscale features. Also, studying the performance of MWA for larger networks and data is an important next step that demands sufficient computational resources.

## References

- [1] Tianping Chen, and Hong Chen. Universal approximation to nonlinear operators by neural networks with arbitrary activation functions and its application to dynamical systems. *IEEE Transactions on Neural Networks* 6, no. 4: 911-917, 1995. [3](#)
- [2] Rewon Child, Scott Gray, Alec Radford, and Ilya Sutskever. Generating long sequences with sparse transformers. *arXiv preprint arXiv:1904.10509* ,2019. [3](#)
- [3] Alexey Dosovitskiy, Lucas Beyer, Alexander Kolesnikov, Dirk Weissenborn, Xiaohua Zhai, Thomas Unterthiner, Mostafa Dehghani et al. An image is worth  $16 \times 16$  words: Transformers for image recognition at scale. *arXiv preprint arXiv: 2010.11929*, 2020. [1, 6](#)
- [4] Amara Graps. An introduction to wavelets. *IEEE computational science and engineering* 2, no. 2 (1995): 50-61, 1995. [4](#)
- [5] John Guibas, Morteza Mardani, Zongyi Li, Andrew Tao, Anima Anandkumar, and Bryan Catanzaro. Efficient token mixing for transformers via adaptive fourier neural operators. In *International Conference on Learning Representations*. 2021. [1, 3, 6](#)
- [6] Kai Han, Yunhe Wang, Hanting Chen, Xinghao Chen, Jianyuan Guo, Zhenhua Liu, Yehui Tang et al. A survey on vision transformer. *IEEE transactions on pattern analysis and machine intelligence* 45, no. 1: 87-110, 2020. [1, 3](#)
- [7] Jonathan Ho, Nal Kalchbrenner, Dirk Weissenborn, and Tim Salimans. Axial attention in multidimensional transformers. *arXiv preprint arXiv:1912.12180*, 2019. [3](#)
- [8] Angelos Katharopoulos, Apoorv Vyas, Nikolaos Pappas, and François Fleuret. Transformers are rnns: Fast autoregressive transformers with linear attention. In *International Conference on Machine Learning*, pp. 5156-5165. PMLR, 2020. [3](#)
- [9] Salman Khan, Muzammal Naseer, Munawar Hayat, Syed Waqas Zamir, Fahad Shahbaz Khan, and Mubarak Shah. Transformers in vision: A survey. *ACM computing surveys (CSUR)* 54, no. 10s: 1-41, 2022. [1, 3](#)
- [10] Nikita Kitaev, Łukasz Kaiser, and Anselm Levskaya. Reformer: The efficient transformer. *arXiv preprint arXiv:2001.04451*, 2020. [3](#)
- [11] M., Barina Kucis, D., Kula, M., & Zemcik, P. 2-D discrete wavelet transform using GPU. In *2014 International Symposium on Computer Architecture and High Performance Computing Workshop* (pp. 1-6). IEEE, 2014. [4](#)
- [12] Juho Lee, Yoonho Lee, Jungtaek Kim, Adam Kosiorek, Seungjin Choi, and Yee Whye Teh. Set transformer: A framework for attention-based permutation-invariant networks. In *International conference on machine learning*, pp. 3744-3753. PMLR, 2019. [3](#)
- [13] James Lee-Thorp, Joshua Ainslie, Ilya Eckstein, and Santiago Ontanon. Fnet: Mixing tokens with fourier transforms. *arXiv preprint arXiv:2105.03824*, 2021. [3](#)
- [14] Zongyi Li, Nikola Kovachki, Kamyar Azizzadenesheli, Burigede Liu, Kaushik Bhattacharya, Andrew Stuart, and Anima Anandkumar. Neural operator: Graph kernel network for partial differential equations. *arXiv preprint arXiv:2003.03485* (2020). [3](#)
- [15] Hanxiao Liu, Zihang Dai, David So, and Quoc V. Le. Pay attention to mlps. *Advances in Neural Information Processing Systems* 34 (2021): 9204-9215. [3](#)
- [16] Meyer, Y. *Wavelets: Algorithms and Applications*, Philadelphia: SIAM (Society for Industrial and Applied Mathematics). *Original French version (1990), Ondelettes, Hermann, Paris*, 1993. [5](#)
- [17] Jack W. Rae, Anna Potapenko, Siddhant M. Jayakumar, and Timothy P. Lillicrap. Compressive transformers for long-range sequence modelling. *arXiv preprint arXiv:1911.05507*, 2019. [3](#)
- [18] Yongming Rao, Wenliang Zhao, Zheng Zhu, Jiwen Lu, and Jie Zhou. Global filter networks for image classification. *Advances in neural information processing systems* 34 (2021): 980-993. [1, 3, 6](#)
- [19] Samir S. Soliman, and Mandyam D. Srinath. Continuous and discrete signals and systems. *Englewood Cliffs* , 1990. [4](#)
- [20] Ibtissam Slimani, Abdelmoghit Zaarane, and Abdellatif Hamdoun. Convolution algorithm for implementing 2D discrete wavelet transform on the FPGA. In *2016 IEEE/ACM 13th International Conference of Computer Systems and Applications (AICCSA)*, pp. 1-3. IEEE, 2016. [4](#)
- [21] Arda Sahiner, Tolga Ergen, Batu Ozturkler, John Pauly, Morteza Mardani, and Mert Pilanci. Unraveling attention via convex duality: Analysis and interpretations of vision transformers. In *International Conference on Machine Learning*, pp. 19050-19088. PMLR, 2022. [3](#)
- [22] Yi Tay, Mostafa Dehghani, Dara Bahri, and Donald Metzler. Efficient transformers: A survey. *ACM Computing Surveys* 55, no. 6: 1-28, 2022. [3](#)
- [23] Hugo Touvron, Piotr Bojanowski, Mathilde Caron, Matthieu Cord, Alaaeldin El-Nouby, Edouard Grave, Gautier Izacard et al. Resmlp: Feedforward networks for image classification with data-efficient training. *IEEE Transactions on Pattern Analysis and Machine Intelligence*, 2022. [3](#)
- [24] Tapas Tripura, Souvik Chakraborty. Wavelet neural operator: a neural operator for parametric partial differential equations. *arXiv preprint arXiv: 2205.02191*. 2022. [1, 4, 5](#)
- [25] Ashish Vaswani, Noam Shazeer, Niki Parmar, Jakob Uszkoreit, Llion Jones, Aidan N. Gomez, Łukasz Kaiser, and Illia Polosukhin. Attention is all you need. *Advances in neural information processing systems* 30, 2017. [1](#)

- [26] Sinong Wang, Belinda Z. Li, Madian Khabsa, Han Fang, and Hao Ma. Linformer: Self-attention with linear complexity. *arXiv preprint arXiv:2006.04768* , 2020. [3](#)
- [27] Tao Wei, Yonghong Tian, and Chang Wen Chen. Rethinking convolution: towards an optimal efficiency. 2020. [6](#)
- [28] Karlton Wirsing. Time frequency analysis of wavelet and Fourier transform. In *Wavelet Theory*. London, UK: IntechOpen, 2020. [4](#), [6](#)
- [29] Jun Zhang, Gilbert G. Walter, Yubo Miao, and Wan Ngai Wayne Lee. Wavelet neural networks for function learning. *IEEE transactions on Signal Processing*, 43(6), 1485- 1497, 1995. [5](#)